P5.8

Aspect Angle Dependence of Outflow Strength in Denver Microbursts: Spatial and Temporal Variations *

Robert G. Hallowell
M.I.T. Lincoln Laboratory
Lexington, Massachusetts 02173

1. INTRODUCTION

MIT Lincoln Laboratory is being sponsored by the Federal Aviation Administration (FAA) to develop and test the Terminal Doppler Weather Radar (TDWR) wind shear surveillance system (Turnbull et al. 1989). As part of this program Lincoln has developed algorithms for automatically detecting microbursts, or thunderstorm outflows using the radial velocity data gathered from a single TDWR. Output from the detection algorithms will be used to warn aircraft of microburst hazards. While the success in automatically detecting microbursts using the Lincoln Laboratory microburst detection algorithm has been encouraging (Merritt et al. 1989), one issue which continues to cause concern is microburst asymmetry. Asymmetry, or aspect angle dependence, in microbursts refers to outflows that have a divergent surface outflow strength or extent that varies depending on the aspect (or viewing) angle of the radar.

The TDWR detection algorithms utilize input from a single Doppler radar; therefore, an asymmetric microburst may be underestimated or go undetected if the radar is viewing the event from an aspect angle where the strength of the outflow is weak. Additionally, the size and location of the event may be distorted when the outflow extent is significantly asymmetric. Most of the present outflow modeling and detection methods are based on the assumption of axial symmetry both in the strength and extent of outflows. Asymmetry in microbursts, therefore, is a major concern for TDWR microburst detection performance.

Past work by Wilson et al. (1984) and Eilts (1987, 1988) has indicated that some microbursts are highly asymmetric, for at least a portion of their lifetime. However, this previous work has been limited in scope to single "snapshots" of the microbursts, generally at their peak outflow strength. Strength asymmetries from these previous studies indicated asymmetry ratios (maximum over minimum strength) ranging from 1.3:1 to as high as 6:1. None of the studies dealt with shape (or extent) asymmetries.

This paper describes the results from a detailed study of 96 individual observations from 27 microburst events. Measurements were taken to determine both the strength and extent of each microburst at multiple aspect angles. The data clearly show that microbursts, on average, have maximum strengths and extents which are 1.9:1 and 1.5:1 asymmetric, respectively.

*The work described here was sponsored by the Federal Aviation Administration. The United States Government assumes no liability for its content or use thereof.

2. DATA

Single-Doppler radar measurements were collected in Denver during 1987 using the FL-2 S-Band (Lincoln Laboratory) and UND C-Band (University of North Dakota) radars. As shown in Figure 1, the UND radar was located 20.3 km north and 1.6 km east of the FL-2 radar. The radar scanning was coordinated to cover microbursts that occurred in favorable dual-Doppler regions. For each scan of an event, the two-dimensional wind field was calculated using the multiple Doppler radar synthesis system suggested by Brown et al. (1981). Surface dual-Doppler wind fields at 250 meter resolution were synthesized from the radar radial velocity fields. The paired radar scans were all surface tilts (0.3°–0.5°) and had time differences of less than 1 minute. In addition the beam intersection angle of the radars had to be greater than 30° and less than 150° (denoted as the shaded area in Figure 1).

The raw two-dimensional wind fields were then smoothed using 3 iterations of a simple 3-by-3 median filter, with 4 of 9 points required to be valid. This smoothing technique had the advantage of filling some small holes in the data without artificially expanding the analysis region greatly. The 10% trimmed mean wind was then removed. A trimmed mean was used to reduce the impact of erroneous wind values on the mean wind. This final perturbation wind field was used for all analyses.

A wide variety of cases were chosen for this analysis to obtain a representative sample of the microbursts found in the Denver environment (Table 1). The "scans" column in Table 1 indicates the number of observations of a particular event, "peak reflectivity" (surface) is listed to show that

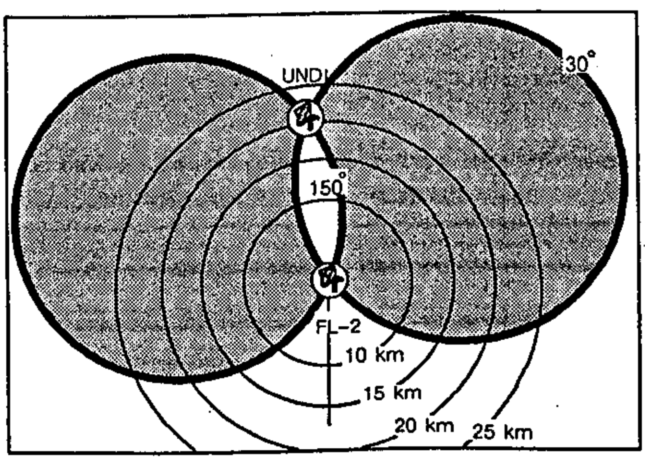

Figure 1. - Relative locations of UND and FL-2. Shaded region denotes valid dual-Doppler region.

both "wet" and "dry" microbursts were examined, and the "maximum strength" indicates the largest differential velocity over all the aspect angles and observations of an event.

2.1. Data Accuracy

The accuracy of the strength estimates used in this analysis is on the order of ±0.5 m/s. However, the layering of polar data to Cartesian grids and the application of a median filter causes a general 15-20% reduction of raw velocity measurements. This reduction is uniform and therefore does not affect the asymmetry statistics presented here. Since the strengths shown here would likely be perceived in raw radar data at slightly higher levels, some weak microburst events (<10m/s) were included in this analysis. Shape estimates have a general accuracy of ±0.35 km.

Table 1. Denver, Co microburst cases used in asymmetry analysis.

Date	Case#	Times(UT)	Scans	Peak Reflect. (dBz)	Max Strength (m/s)
7/16	1	2306-2320	5	15	24
	2	2307-2313	4	13	26
7/28	3	2320-2235	8	31	16
	4	2220-2233	8	36	15
	5	2220	1	12	10
	6	2224	1	34	16
	7	2241-2243	3	49	16
	8	2248-2250	3	54	24
	9	2256-2257	2	49	18
7/31	10	2251	1	4	17
	11	2251-2256	5	43	10
	12	2252-2256	4	38	8
	13	2255-2301	6	38	13
	14	2259-2300	2	35	10
8/2	15	2243-2247	5	28	10
	16	2247-2257	11	33	13
	17	2252	1	10	12
8/6	18	2025-2030	6	16	10
	19	2026-2029	4	16	11
9/3	20	2135-2145	3	31	14
	21	2145	1	13	10
	22	2145	1	5	15
	23	2150-2200	3	27	18
	24	2200-2205	2	20	15
	25	2200	1	0	8
9/4	26	2015-2018	2	23	15
9/11	27	0258-0308	3	56	24

3. ANALYSIS METHODOLOGY

Figure 2 illustrates the velocity trace along a line segment passing through the center of a microburst. The segment between the start and stop arrows indicates a region where the radial velocity is generally increasing (i.e., a region of positive or divergent shear). To find these regions of divergent microburst outflow, the perturbation wind field was examined visually, and a bounding polygon was subjectively drawn around each microburst region.

In general, the sides of the polygon were drawn to enclose the region of positive shear discussed above. The shape of the polygon was used to determine the outflow extent of the microburst, and was therefore important in the calculation of microburst shape statistics. The polygons for isolated microbursts (single distinct outflows) were fairly easy to define. Complicated multi-cell or line microbursts, such as those discussed by Hjemfelt (1985), were much harder to define using a single polygon. Consequently, only the portions of the overall flow which had distinct edges

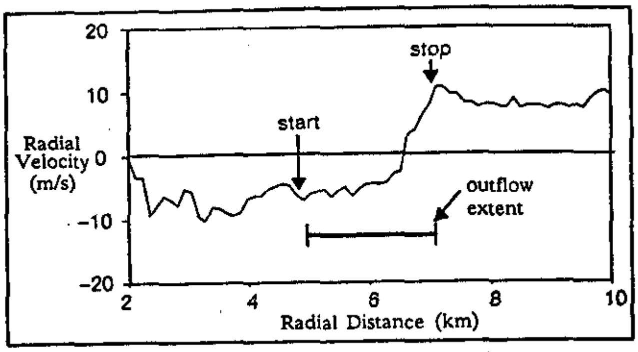

Figure 2. Typical velocity profile through microburst center.

(surrounded by regions of convergence) were identified and analyzed for multi-cell and line microbursts.

Once an event was drawn, the velocity difference across every unique gridpoint pair within the polygon was calculated, taking into account the relative aspect angle of the segment. Note that the differential velocity measurement was calculated between two points; no shear threshold was set for the intervening points. The strength calculations were only performed on points whose connecting lines were completely contained within the defined polygon. It was assumed that points within the polygon were generally divergent because the sides of the polygon limit the strength analysis to the microburst outflow region.

The relative aspect angle of the line formed by each pair of gridpoints was determined by placing a fictitious radar 15 km from the centroid of the polygon. As shown in Figure 3, the radar which has a beam parallel to the test segment within the polygon (thick line on figure) defines the aspect angle of that segment. In the example shown the aspect angle of the segment is 130° (relative to the event polygon, not the radar).

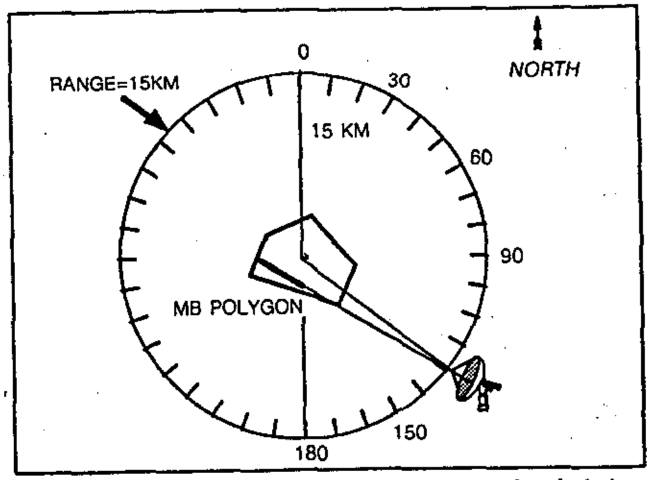

Figure 3. Diagram illustrating relative aspect angle calculations for asymmetry analysis.

Differential velocity and shape measurements were obtained from all possible aspect angles and then grouped into one of eighteen aspect angle categories. The categories ranged from 0°±5°(due North), to 170°±5° in ten degree steps. Aspect angles over 180° were not considered because they generally reflect measurements made from 0°–180°

(though not exactly due to the way relative aspect angles were calculated). Other statistics such as mean wind and peak reflectivity (magnitude, extent and location) were also measured.

4. TYPES OF ASYMMETRY

The TDWR system is designed to identify the location and size of a microburst and estimate the maximum differential velocity of the event. Figure 4 shows the dual-Doppler wind field for a microburst that is nearly symmetric in strength and shape. A Doppler radar would find roughly the same strength, location, and size for this event, regardless of its viewing angle. This is the kind of symmetry which, in general, is currently assumed to exist for all microbursts. However, there are primarily two types of asymmetry that may occur in microbursts: strength and shape.

4.1. Strength Asymmetry

The strength asymmetry of an event is measured by estimating the largest differential velocity within the microburst outflow at multiple aspect angles. Differential velocity is the magnitude of the wind change between any two points within the event. The severity of the aspect angle dependence for strength in an observation may be measured by dividing the maximum strength by the minimum strength over all aspect angles. A strength asymmetry ratio of 1.0 would indicate a microburst perfectly symmetrical with respect to strength. The observation shown in Figure 4 has a strength asymmetry of only 1.3:1 (20m/s ÷ 15m/s).

A single-Doppler radar will, in general, underestimate the maximum strength of a microburst strongly asymmetric in strength. The dual-Doppler wind field shown in Figure 5 reveals a microburst with a strength asymmetry ratios of 2.3:1. The differential velocity trace over all aspect angles is given in the graph directly above the wind field. Figure 6 shows the contours of radial velocity for a radar viewing from the maximum strength aspect angle (0°) and located 15 km from the centroid of the event shown in Figure 5. Similarly, Figure 7 shows the radial velocity contours for a radar radially aligned with the angle of weakest strength (90°). Note that the velocity field from the peak viewing angle indicates a strong shear region with a peak velocity differential of 24.3 m/s. The radial velocity field from the weak viewing angle, on the other hand, yields a weak radially skewed velocity couplet with peak radial velocity of only 10.4 m/s. The "skewed couplet" is a common occurrence in any asymmetric microburst; unfortunately, it may occur at any aspect angle (not just the minimum strength angle) and therefore gives little insight on the true asymmetry of the event (Eilts 1988).

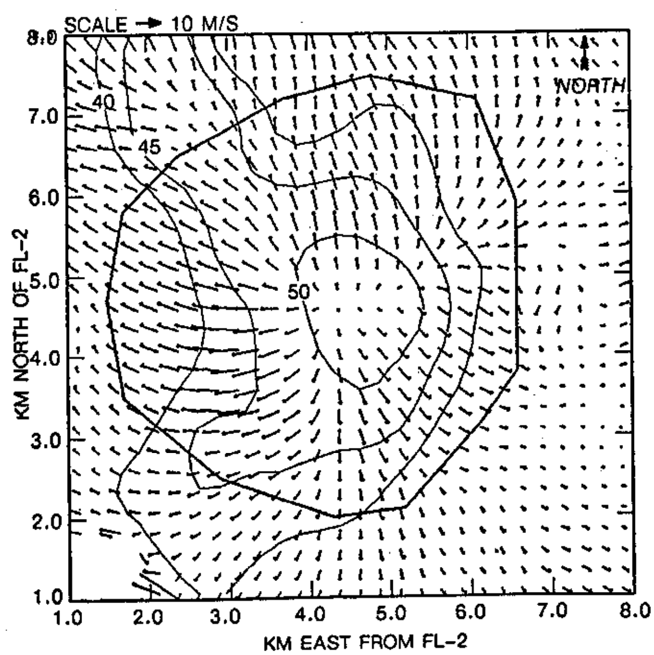

Figure 4. Dual-Doppler wind field for a shape and strength symmetric microburst on July 28, 1987 at 22:48:27 UT. Polygon for event shown in center; contoured lines are of reflectivity at 40, 45, and 50 dBz.

4.2. Shape Asymmetry

The shape asymmetry of an event is measured by estimating the largest spatial extent of the microburst outflow at multiple aspect angles. The shape of an event (outflow extent) is measured by estimating the cross-distance from one end of the outflow polygon to the other at a variety of aspect angles. The level of aspect angle dependence for outflow extent is calculated by dividing the largest cross-distance by the smallest cross-distance over all aspect angles. The event shown in Figure 4 has a shape asymmetry of 1.2:1 (5.5km ÷ 4.5km).

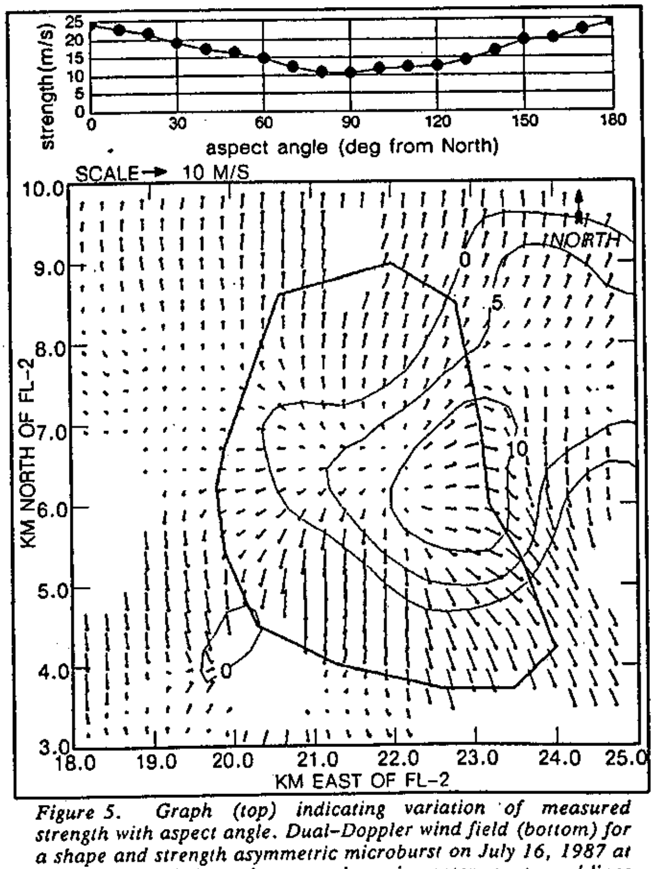

Figure 5. Graph (top) indicating variation of measured strength with aspect angle. Dual-Doppler wind field (bottom) for a shape and strength asymmetric microburst on July 16, 1987 at 23:07:41 UT. Polygon for event shown in center; contoured lines are of reflectivity at 0, 5, and 10 dBz.

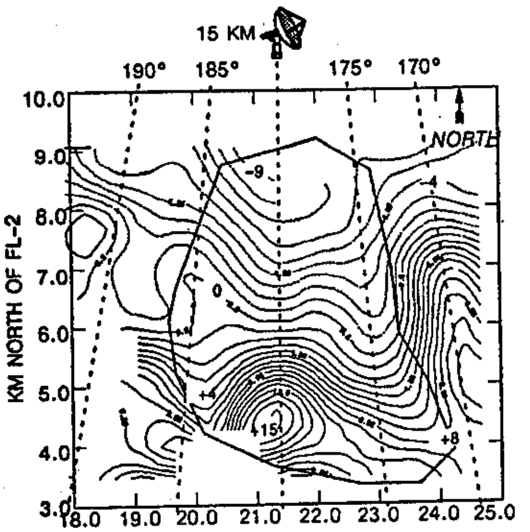

Figure 6. Contours of the radial velocity field (1m/s intervals) extracted from dual-Doppler wind field in Figure 5 relative to a fictitious radar located at a range of 15 km and an azimuth of 0°.

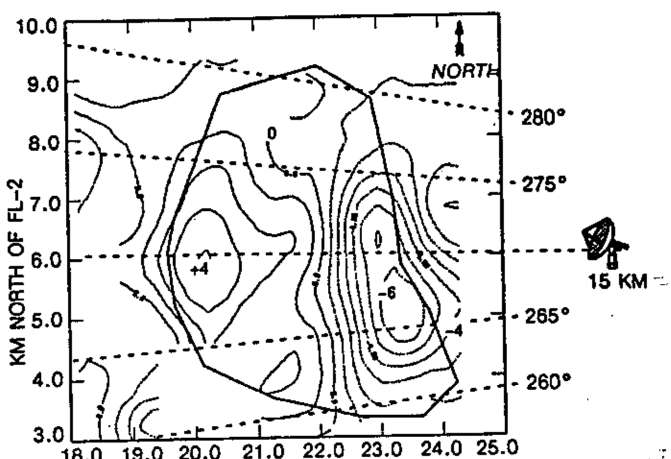

Figure 7. Contours of the radial velocity field (1m/s intervals) extracted from dual-Doppler wind field in Figure 5 relative to a fictitious radar located at a range of 15 km and an azimuth of 90°.

A highly aspect-angle-dependent outflow shape makes it difficult to capture the shape, and sometimes central location, of the microburst using a single-Doppler radar. For example, the observation in Figure 5 has a shape asymmetry of 1.7:1. If we reexamine the radial velocity fields shown in Figure 6 and Figure 7, we see differences in not only the strengths of the fields, but also the location of the peak strengths. Further, the extent of the event (searching for radials where the strength is a fixed percentage of the peak at that angle) is significantly different in size and shape. Part of this difference is caused by the strength asymmetry, but a major portion is caused by the elongated physical shape of the outflow.

5. CHARACTERISTICS OF ASYMMETRY

The characteristics of asymmetry may be divided into two categories: general and event lifetime. The general characteristics are compiled using all the observations listed in Table 1. Lifetime characteristics are based only on the events in Table 1 having more than 4 scans of the event.

5.1. General Characteristics

The events chosen for this analysis were randomly chosen from those available during 1987 Denver operations and, as such, the distribution of maximum event strengths is similar to that found by Biron & Isaminger (1988). The maximum and minimum strengths for each observation are shown in Figure 8. The aspect angle dependence of strength for all events is between 1.3:1 and 3.8:1, with a median value of 1.9:1. As shown in Figure 9, this cumulative probability does not change significantly between weak (thin solid line) and moderate-strong (dotted line) events.

The maximum and minimum outflow extents for each microburst observation are shown in Figure 10. Shape asymmetry ratios for all events range from 1.1:1 to 2.4:1, with a median value of 1.55:1. As for strengths, the cumulative frequency of shape asymmetry ratios, as shown in Figure 11, does not vary significantly between weak (thin solid line) and moderate-strong (dotted line) events.

Figure 9 and Figure 11 (and further statistical analyses not discussed here) indicate that the maximum strength of an event has little or no correlation with the degree of the strength or shape asymmetry. Additionally, the two forms of asymmetry are statistically unrelated. High or low strength asymmetry ratios are equally as likely to have high or low shape asymmetry ratios and vice-versa. None of the microbursts parameters (mean wind speed, peak reflectivity, strength, etc.) analyzed during this study showed significant correlation to the strength or shape asymmetry of individual observations.

In most instances, the azimuth angles of the maximum strength and extent showed no preferred orientation with respect to the environment or each other. The exception to this was for those events with both high strength (>2.3) and shape (>1.75) asymmetry ratios, for which orientation angles tended to be co-located (i.e., the peak strength occurred along the largest cross-distance). However, the lim-

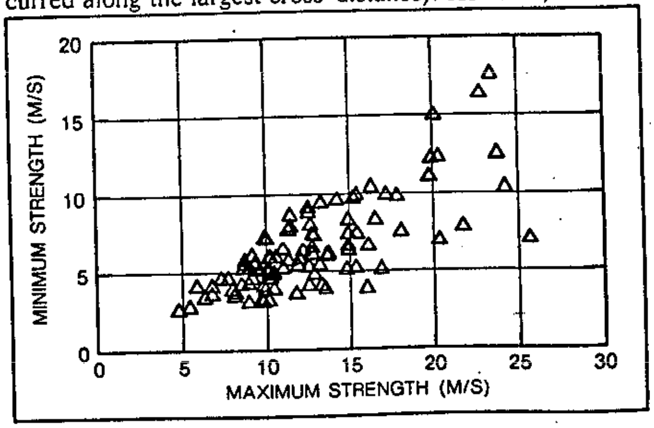

Figure 8. Scatter diagram illustrating spread of maximum and minimum strengths for each observation.

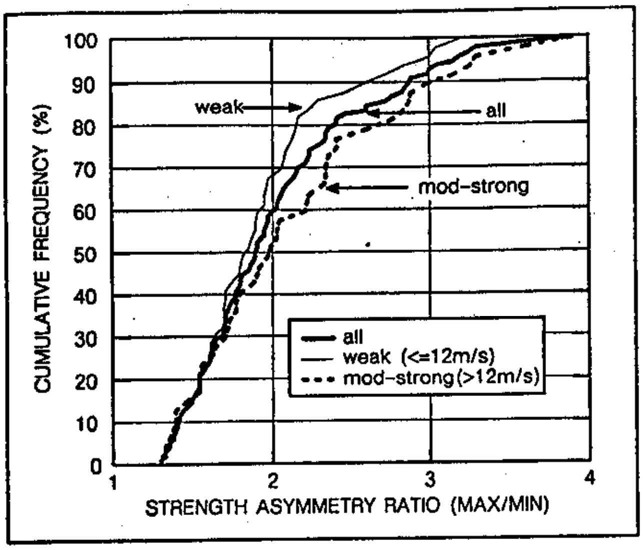

Figure 9. Cumulative frequency of strength asymmetry ratios for various maximum strength classes.

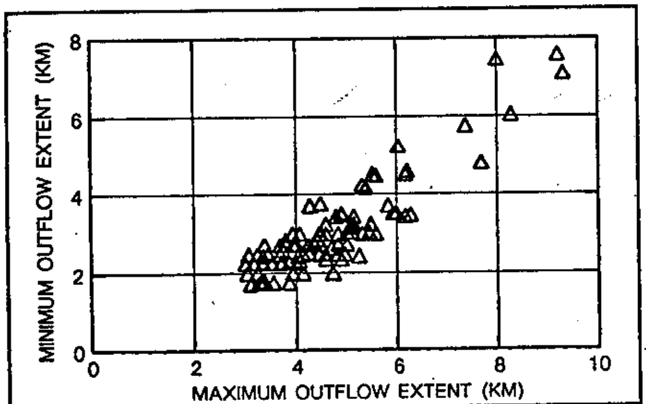

Figure 10. Scatter diagram illustrating spread of maximum and minimum outflow lengths for each observation.

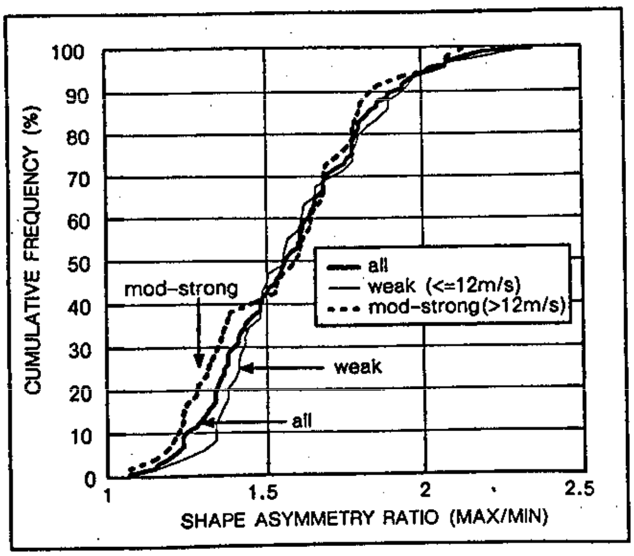

Figure 11. Cumulative frequency of shape asymmetry ratios for various maximum strength classes.

ited number of cases which met this criteria makes the reliability of this correlation uncertain.

5.2. Lifetime Characteristics

There were only seven events which had more than 4 dual-Doppler scans, and were thus suitable for analysis of lifetime characteristics. This is a limited data set, but large enough to provide some estimate of the broad changes in asymmetry over an event's lifetime.

The orientation angle of both the maximum strength and maximum cross-distance remains relatively constant ($\pm 10°$) over the lifetime of the microburst. This is important in that a radar which is viewing an asymmetric event from an unfavorable angle (with respect to strength) will continue to underestimate the strength of the event unless it moves into a more favorable position. At a range of 15 km, an event would need to move approximately 3 km to change the viewing angle by 10° (assuming motion is not directly away from or toward the radar). For the seven event lifetimes analyzed, the microbursts traveled a total distance (based on the polygon centroid) of between 1 and 5 km. This small movement would not likely be sufficient to obtain a more favorable viewing angle.

The magnitude of the strength or shape asymmetry for isolated events tended to remain stable throughout the event's history. However, environmental influences (other microbursts, gust fronts, minor divergences) appeared to cause significant fluctuations in the magnitude of the asymmetry over time.

6. INDICATIONS OF ASYMMETRY

The assumption has generally been made that microbursts are symmetric events. The data presented here clearly indicate that this is not the case. Perhaps a better representation of microburst strength and shape is an ellipse (formed by the maximum and minimum strength or extent of the event). If an ellipse were used to represent microburst outflows, then a parameter P (strength or shape) may be predicted at any aspect angle ϕ using the formula in Figure 12.

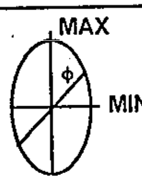

$$P_\phi = \frac{MAX}{\sqrt{\left(\left(\frac{MAX}{MIN}\right)^2 - 1\right)\sin^2(\phi) + 1}}$$

Figure 12. Formula for the elliptical distribution of strength and shape parameters.

This formula was applied to all the microburst observations. Figure 13 shows a scatter diagram of the measured strength versus the strength predicted with this formula for all observations and aspect angles. The overall correlation for all aspect angles was 0.92 for strength and 0.96 for shape (not shown). The angle between the maximum and minimum strength orientation angles is 70°–90° in over 70% of the cases, and the same was true for cross-distances. An elliptical representation of microburst strength and shape parameters gives a surprisingly good fit over a wide range of strengths and extents.

A non-aspect angle dependent measure of the orientation of this ellipse would clearly be helpful. As noted earlier, none of the parameters examined in this analysis were found to indicate the orientation or degree of the asymmetry. In most cases, asymmetry appeared to be a function of the location of the microburst relative to other microbursts or weak divergence regions. Strong outflows would push into weak outflows, thereby distorting the flow of the weaker event. Observationally, isolated microbursts appear to be more symmetric than line or multiple microbursts. However, even isolated microbursts have some asymmetry which appears to be, in part, a function of the complexity of the environmental flow.

7. FUTURE WORK

While the analysis presented above is sufficient to describe microburst asymmetry in Denver's unique weather environment, microbursts from other regions of the country should also be examined. The TDWR testbed from which the data were taken operated in Kansas City, MO during 1989, and is currently operating in Orlando, FL. These data should be examined for asymmetry to confirm or modify the results presented here.

The point-to-point method of calculating differential velocity, while simple to implement and efficient to use, requires the assumption that intervening wind data points are divergent. Careful scrutiny of both the wind fields and event polygons helps to reduce any potential analysis problems. In the future, however, it may be beneficial to search for line "segments" within the polygon which have generally positive shear along their length.

Finally, the mechanism for creating asymmetry needs to be understood. The environmental flow, proximity and orientation to other events, and even the topography of the land underlying microburst may be a factor. A thorough analysis of the interaction of microbursts with their surrounding environmental flow would be worthwhile. A comparison of Denver, CO (sloping terrain) and Orlando, FL (flat wetlands) may yield some insight on the effect of terrain on asymmetry.

8. SUMMARY & CONCLUSIONS

Over 27 events encompassing 96 total observations of microbursts were examined for asymmetry. There were two types of asymmetry which were studied: strength and shape. The median strength and shape asymmetry ratios, for the cases presented here, were 1.9:1 and 1.55:1, respectively. The representation of microbursts as symmetric flows is clearly inaccurate.

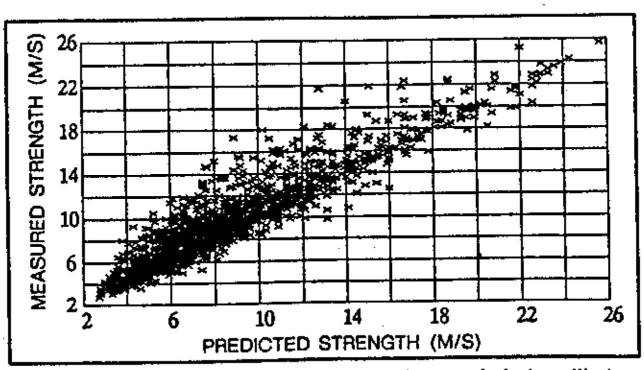

Figure 13. Scatter diagram of predicted strength (using elliptical model) vs. measured strength for all observations and aspect angles.

The magnitude of the shape and strength asymmetry ratios were found to be independent of the magnitudes of the maximum cross-distance (shape) and strength measurements. No preferred orientation angles were found for maximum strength or shape, although the orientation angles did remain relatively stable throughout the lifetime of the events.

Based on these findings, a single-Doppler radar has an equal chance of viewing a microburst of all sizes and strengths from any random aspect angle. Therefore, the radar will underestimate the overall maximum strength of the event, on average, by approximately 30% (based on median strength asymmetry ratio of 1.9:1). The primary cause of asymmetry (or at least fluctuations in its magnitude) in microbursts appears to be the proximity of other wind shear events (gust fronts, microbursts, or weak divergences). There appear to be no reliable, single Doppler-radar based measurements (reflectivity, peak radial strength, mean wind, etc.) which indicate the severity or orientation of asymmetry in microbursts.

ACKNOWLEDGEMENTS

The author wishes to thank Mark Isaminger for his efforts in processing the dual-Doppler wind fields, Mark Merritt for his general supervision and analytical insights, and, Dr. James Evans, Dr. Marilyn Wolfson, Dave Clark, and Leslie Mahn for their editorial and meteorological comments and suggestions.

REFERENCES

Biron, Paul J., and Isaminger, Mark A., 1989: An analysis of microburst characteristics related to automatic detection from Huntsville, AL and Denver, CO. Preprints, 24th Conference on Radar Meteorology, Tallahassee, FL, *American Meteorological Society*, pp. 269–273.

Brown, et al., 1981: Multiple Doppler radar analysis of severe thunderstorms: designing a general analysis system. NOAA Technical Memorandum ERL-NSSL-92.

Eilts, Michael D., 1988: Use of a single Doppler radar to estimate the runway to wind shear component in microburst outflows. 26th Aerospace Sciences Meeting Paper, Jan., 1988, *American Institute of Aeronautics and Astronautics*, AIAA-88-0694.

Eilts, Michael D., and Doviak, Richard J., 1987: Oklahoma downbursts and their asymmetry. *Journal of Climate and Applied Meteorology*, vol. 26, pp. 66–78.

Hjemfelt, M.R., and Roberts, R.D., 1985: Microburst lines. Preprints, 14th Conference on Severe Local Storms, Indianapolis, Indiana, *American Meteorological Society*, pp. 297–300.

Merritt, Mark W., et al., 1989: Wind shear detection with pencil-beam radars. *The Lincoln Laboratory Journal*, Volume 2, Number 3, pp. 483–510.

Turnbull, D., J. McCarthy, J. Evans, D. Zrnic', 1989: The FAA Terminal Doppler Weather Radar (TDWR) program. Preprints, *3rd International Conference on the Aviation Weather Systems*, Anaheim, CA, pp. 414–419.

Wilson, et. al., 1984: Microburst wind shear and evaluation of Doppler radar for airport wind shear detection. *Journal of Climate and Applied Meteorology*, vol. 23, pp. 898–915.